Structure and electrical transport properties of the ordered skutterudites $MGe_{1.5}S_{1.5}$ (M = Co, Rh, Ir)

Paz Vaqueiro*, Gerard G. Sobany, Martin Stindl

Department of Chemistry, Heriot-Watt University, Edinburgh EH14 4AS, UK

Abstract

High-resolution powder neutron diffraction data collected for the skutterudites $MGe_{1.5}S_{1.5}$ (M = Co, Rh, Ir) reveal that these materials adopt an ordered skutterudite structure (space group $R\bar{3}$), in which the anions are ordered in layers perpendicular to the [111] direction. In this ordered structure, the anions form two-crystallographically distinct four-membered rings, with stoichiometry Ge_2S_2, in which the Ge and S atoms are *trans* to each other. The transport properties of these materials, which are p-type semiconductors, are discussed in the light of the structural results. The effect of iron substitution in $CoGe_{1.5}S_{1.5}$ has been investigated. While doping of $CoGe_{1.5}S_{1.5}$ has a marked effect on both the electrical resistivity and the Seebeck coefficient, these ternary skutterudites exhibit significantly higher electrical resistivities than their binary counterparts.
© 2008 Published by Elsevier Inc.

Keywords: Ternary skutterudite; Thermoelectric properties; Neutron diffraction

1. Introduction

Materials with the general formula MX_3 (M = Co, Rh, Ir and X = P, As, Sb; M = Ni, Pd; X = P) [1–3] crystallise in the skutterudite structure, which can be considered as a severe distortion (tilt system $a^+a^+a^+$) of the ReO$_3$ structure (Fig. 1(a)) [4]. The skutterudite structure can be derived from that of ReO$_3$ by distortion of the anion sublattice. This is achieved by displacing four of the anions located at the ReO$_3$ unit cell edges towards its centre, as shown in Fig. 1(b), and results in the formation of the characteristic four-membered X_4 rings of the skutterudite structure. The new unit cell (Fig. 1(c)), which is body-centred (space group $Im\bar{3}$) has eight times the volume of the original ReO$_3$ unit cell ($a = 2a_p$), and while the cations retain their octahedral coordination, the anions are located in a distorted tetrahedral environment, coordinated by two cations and two anions. The skutterudite structure is closely related to ordered double perovskites of the type $AA_3'B_4X_{12}$ (e.g. CaCu$_3$Ti$_4$O$_{12}$) [4,5]. When the A- and

A'-sites are vacant the skutterudite structure ($\square\square_3B_4X_{12} \equiv BX_3$) is obtained, while materials in which the A-site is partially occupied are known as filled skutterudites, $A_x\square_3B_4X_{12}$ ($0 < x \leqslant 1$; A = La–Yb, U, Th, Tl; B = Fe, Ru, Os; X = P, As, Sb) [6–8]. In recent years, materials with the skutterudite structure have attracted increasing attention owing to their potential for high-temperature thermoelectric applications [9–11], as well as for the interesting physical phenomena found in the rare-earth filled skutterudites, such as metal–insulator transitions [12] and superconductivity [13].

Our recent efforts have centred on the preparation and characterisation of ternary skutterudites, which are materials isoelectronic to the binary skutterudites. Ternary skutterudites can be obtained either by substitution at the anion site, X, by a pair of elements from groups 14 and 16 (e.g. $CoGe_{1.5}S_{1.5}$) [14], or by isoelectronic substitution at the cation site, M, by a pair of elements from groups 8 and 10 (e.g. Fe$_{0.5}$Ni$_{0.5}$Sb$_3$) [15]. Although a number of ternary skutterudites have been reported [14–19], there has been limited work to date on the structure and properties of these materials. While ternary skutterudites formed by cation substitution appear to be isostructural to

*Corresponding author. Fax: +44 131 451 3180.

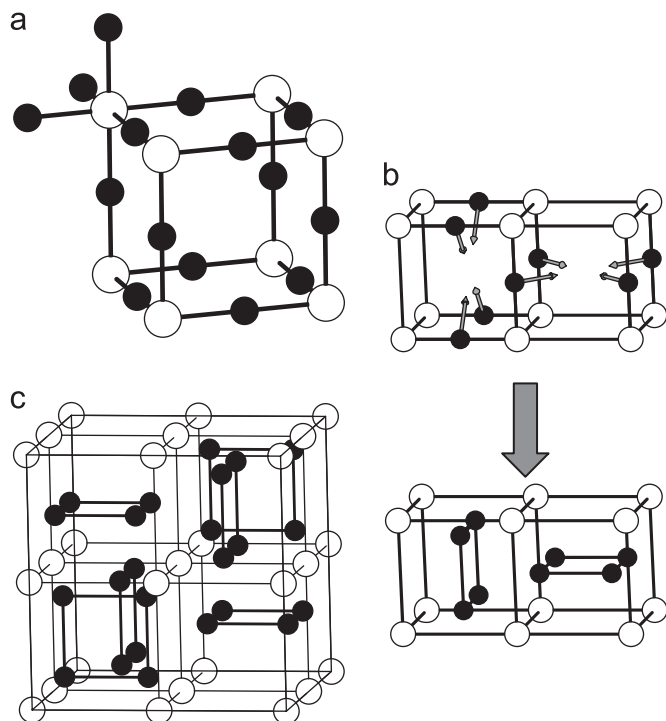*E-mail address:* chepv@hw.ac.uk (P. Vaqueiro).

Fig. 1. (a) The ReO_3 structure, showing the octahedral coordination of one of the metal atoms, (b) a fragment of the ReO_3 structure, showing the distortion of the anion sublattice which results in the skutterudite structure, and (c) the skutterudite structure, with its characteristic anion rings. Unit cell is outlined. Key: metal atoms, open circles; anions, black circles.

the binary skutterudites [15,18], a detailed structural study on $CoGe_{1.5}Te_{1.5}$ concluded that the anions are ordered in layers perpendicular to the [111] direction of the skutterudite unit cell [20]. The known ternary skutterudites obtained by isoelectronic substitution at the anion site have been summarised in Ref. [20]. We report here a structural study of the ternary skutterudites $MGe_{1.5}S_{1.5}$ (M = Co, Rh, Ir), carried out using high-resolution powder neutron diffraction, together with their electrical transport properties. As it has been found [9,10] that in binary skutterudites such as $CoSb_3$, substitution of a small fraction of Co with Fe or Ni has a marked effect on the transport properties, we have also investigated the effect of doping on the electrical transport properties of $CoGe_{1.5}S_{1.5}$, by preparing samples of $Co_{1-x}Fe_xGe_{1.5}S_{1.5}$ ($0 < x \leqslant 0.1$).

2. Experimental

Mixtures of the elements corresponding to the stoichiometry $MGe_{1.5}S_{1.5}$ (M = Co, Rh, Ir) were ground in an agate mortar prior to sealing into an evacuated ($< 10^{-4}$ Torr) silica tube. Ge powder was reduced in a stream of H_2/N_2 at 500 °C to remove GeO_2 prior to use. The inner wall of the silica tubes was coated with a thin layer of carbon by pyrolysis of acetone, in order to avoid reaction of the reaction mixture with the silica walls. For the preparation of $CoGe_{1.5}S_{1.5}$, the reaction mixture was heated at 500 °C

for 2 days and then cooled to room temperature at 0.5 °C min^{-1} prior to removal from the furnace. Following re-grinding, the material was sealed into a second silica tube, refired at 700 °C for 5 days, and cooled to room temperature at 0.1 °C min^{-1}. For the synthesis of $RhGe_{1.5}S_{1.5}$ and $IrGe_{1.5}S_{1.5}$, the reaction mixtures were heated at 500 °C for 1 day, 700 °C for 1 day and finally at 800 °C for 2 days. After cooling at 0.5 °C min^{-1} to room temperature, the materials were ground, sealed into a second silica tube, heated at 800 °C for 2 days and then slow cooled to room temperature, with a cooling rate of 0.5 °C min^{-1}. To investigate the effect of doping on the electrical transport properties, samples of $Co_{1-x}Fe_xGe_{1.5}S_{1.5}$ ($0 < x \leqslant 0.1$) were prepared using a similar procedure to that used for the stoichiometric phase. The samples were initially characterised using powder X-ray diffraction, collected on a Philips PA2000 diffractometer with nickel-filtered Cu-$K\alpha$ radiation ($\lambda = 1.5418$ Å). For transport property measurements, pellets of $MGe_{1.5}S_{1.5}$ were cold pressed, sealed into an evacuated silica tube, heated at 700–800 °C for 1 or 2 days and then cooled to room temperature at 0.5 °C min^{-1}. Transport property measurements for $IrGe_{1.5}S_{1.5}$ were omitted as it was found that this material contains a large amount of unreacted Ir and IrGe. The sulphur content was determined thermogravimetrically by oxidation in a flow of dry oxygen on a Du Pont Instruments 951 Thermogravimetric Analyzer.

Time-of-flight powder neutron diffraction data were collected on the HRPD diffractometer at ISIS, Rutherford Appleton Laboratory. The samples were contained in vanadium slab cans, and data were collected at 4.2 and 293 K for M = Co, Rh but only at 293 K for $IrGe_{1.5}S_{1.5}$. Initial data manipulation and reduction was carried out using Genie [21] spectrum manipulation software. Neutron diffraction data from the backscattering and 90° detector banks were summed, normalised and used simultaneously in Rietveld refinements, which were performed using the GSAS package [22]. Data from the samples containing Rh and Ir were corrected for absorption.

The electrical resistance of the samples as a function of temperature ($77 \leqslant T/K \leqslant 400$) was measured using the 4-probe DC technique. Ingots ($\sim 6 \times 3 \times 1$ mm^3) were cut from sintered pellets ($> 75\%$ of the theoretical density), four 50 μm silver wires were attached using colloidal silver paint and connections were made to a HP34401A multimeter. The samples were mounted in an Oxford Instruments CF1200 cryostat connected to an ITC502 temperature controller. Measurements of the Seebeck coefficient in 5 K steps over the temperature range $70 \leqslant T/K \leqslant 380$ were made on ingots (ca. $8 \times 4 \times 1$ mm^3) cut from sintered pellets. Each sample ingot was mounted on a copper holder, which incorporates a small heater (120 Ω strain gauge) located close to one end of the sample. The copper holder is attached to the hot stage of a closed-cycle refrigerator (DE-202, Advanced Research Systems), which is connected to a Lakeshore LS-331 temperature controller. Two 50 μm copper wires were attached to the ends of the

sample using silver paint and connections made to a Keithley 2182A nanovoltmeter. Two Au: 0.07% Fe vs. chromel thermocouples were placed close to the sample at the hot and cold ends, and connected to a second Lakeshore LS-331 temperature controller. The Seebeck coefficient at a given temperature was determined by applying a temperature gradient, ΔT, across the sample and measuring the corresponding thermal voltage, ΔV. The slope of the line, $\Delta V/\Delta T$, was used to determine the Seebeck coefficient.

3. Results and discussion

Powder X-ray diffraction data were consistent with the formation of single-phase materials and could be indexed on the basis of a primitive cubic unit cell, with the intense reflections corresponding to the skutterudite body-centred condition $h+k+l = 2n$. The lattice parameter, a, increases with increasing the size of the transition metal, while for the doped $Co_{1-x}Fe_xGe_{1.5}S_{1.5}$ phases, the lattice parameter increases slightly with increasing iron content. The results of the thermogravimetric analysis presented in Table 1 indicate generally good agreement between nominal compositions and those determined analytically. However, subsequent examination of powder neutron diffraction data indicated that, despite the precautions taken to avoid the presence of germanium oxide, all prepared materials contain small amounts of GeO_2 and binary sulphides, while the $IrGe_{1.5}S_{1.5}$ sample contains significant amounts of IrGe (ca. 11%) and Ir (ca. 3%).

3.1. Structural analysis

While laboratory X-ray diffraction data are consistent with a primitive cubic unit cell, peak splittings are apparent in the high-resolution neutron diffraction data collected for $RhGe_{1.5}S_{1.5}$, suggesting that the symmetry is lower than cubic. Previous studies on ternary skutterudites formed by anion substitution also point to a lower symmetry. For instance, Guinier photographs collected on $RhGe_{1.5}S_{1.5}$ by Lutz and Kliche [17] were indexed on the basis of a rhombohedral unit cell. Korenstein et al. [14] reported that the structure of $CoGe_{1.5}S_{1.5}$ could be described in the noncentrosymmetric space group $R3$ by taking into account short-range ordering of the anions, whilst Partik et al. [23] carried out a single-crystal study on twinned crystals of $CoGe_{1.5}Q_{1.5}$ ($Q = S$, Se) and reported that the Ge and Q atoms exhibit long-range ordering, which results in a lowering of the symmetry from cubic to rhombohedral (space group $R3$). However, use of Platon/Addsym to identify missing symmetry elements [24,25], in the two reported structures of $CoGe_{1.5}S_{1.5}$ [14,23] indicated clearly that there was a centre of inversion missing, and that therefore this structure should be better described in the centrosymmetric space group $R\bar{3}$. Following the group theoretical analysis described in Ref. [20], Rietveld refinements using the neutron diffraction data were carried out

Table 1
Results of thermogravimetric analysis

Nominal composition	Expected TGA weight gain (%)	Experimental TGA weight gain (%)	Experimental composition
$CoGe_{1.5}S_{1.5}$	11.07	10.66	$CoGe_{1.5}S_{1.52}$
$Co_{0.95}Fe_{0.05}Ge_{1.5}S_{1.5}$	11.08	10.52	$Co_{0.95}Fe_{0.05}Ge_{1.5}S_{1.53}$
$Co_{0.90}Fe_{0.10}Ge_{1.5}S_{1.5}$	11.09	10.42	$Co_{0.90}Fe_{0.10}Ge_{1.5}S_{1.54}$
$RhGe_{1.5}S_{1.5}$	6.12	6.40	$RhGe_{1.5}S_{1.48}$

in the space group $R\bar{3}$. A region centred at $d\sim2.2$ Å was excluded from the neutron data, owing to the presence of features due to instrumental vanadium ($d = 2.141$ Å). For all $MGe_{1.5}S_{1.5}$ phases, refinements carried out in $R\bar{3}$ resulted in a significantly better agreement between observed and calculated data than those carried out in the ideal skutterudite structure ($Im\bar{3}$). After refinement of background terms, peak shape parameters, phase fractions, lattice parameters, thermal parameters and atomic parameters, it became evident that the sulphur atoms had very small thermal parameters when compared to the remaining atoms. This suggested that partial disorder between the Ge and S sites may occur, as previously indicated by Korenstein et al. [14] and therefore anion site occupancy factors were introduced as variables into these refinements, with the constraint that the overall stoichiometry is maintained. The partially disordered model resulted in a better agreement between observed and calculated data, reflected in lower R_{wp} values (for 90° bank data, $R_{wp} = 3.4$–4.7% for the fully ordered model, while $R_{wp} = 3.1$–4.3% for the partially disordered model). The final refinements indicate that a small percentage of S atoms reside on the Ge sites and viceversa (2.5%, 0.6% and 5.6% for $M =$ Co, Rh and Ir, respectively). The refined parameters for the structures of $MGe_{1.5}S_{1.5}$ in the space group $R\bar{3}$ are presented in Table 2, while final observed, calculated and difference profiles for the neutron diffraction data at room temperature are shown in Fig. 2. Selected distances and angles are given in Table 3.

The structure of $MGe_{1.5}S_{1.5}$ can be described as an infinite array of distorted and tilted octahedra, with each octahedron sharing corners with six neighbouring octahedra (Fig. 3(a)). This structure retains the $a^+a^+a^+$ tilt system of the parent skutterudite structure, while the anions are ordered in layers perpendicular to the [111] direction of the skutterudite unit cell (Fig. 3(b)). Each M cation has a distorted octahedral coordination to three germanium and three sulphur atoms, with the anions arranged in a facial configuration, in which each type of anion defines one face of the octahedron. The octahedral bond length distortion [26] is larger for $CoGe_{1.5}S_{1.5}$ than for the other two members of the series. The X–M–X angles deviate significantly from 90° (Table 3), with values over the range 99.2(4)–83.54(25)° for $CoGe_{1.5}S_{1.5}$ at room temperature and similar deviations for the remaining phases. The tilt angle (ϕ) for the ideal skutterudite structure

Table 2
Refined parameters for the ordered skutterudites $MY_{1.5}Q_{1.5}$ (space group $R\bar{3}$)

		CoGe$_{1.5}$S$_{1.5}$		RhGe$_{1.5}$S$_{1.5}$		IrGe$_{1.5}$S$_{1.5}$
		4.2 K	293 K	4.2 K	293 K	293 K
a (Å)		11.32287(6)	11.33902(7)	11.67841(9)	11.69416(6)	11.72719(8)
c (Å)		13.8882(2)	13.9066(2)	14.3646(2)	14.3820(1)	14.4145(2)
$M(1)$[a]	z	0.258(1)	0.258(1)	0.2519(7)	0.2512(3)	0.2529(4)
	B (Å^2)	0.33(6)	0.64(4)	1.26(3)	0.81(2)	0.72(2)
$M(2)$	x	0.673(2)	0.670(2)	0.666(1)	0.6675(6)	0.6683(6)
	y	0.839(1)	0.8378(9)	0.8318(6)	0.8321(3)	0.8334(4)
	z	0.5889(4)	0.5893(4)	0.5855(3)	0.5864(2)	0.5857(1)
	B (Å^2)	0.33(6)	0.64(4)	1.26(3)	0.81(2)	0.72(2)
$Y(1)$	SOF Ge	0.973(1)	0.975(1)	0.996(1)	0.995(1)	0.944(3)
	SOF S	0.027(1)	0.025(1)	0.004(1)	0.005(1)	0.056(3)
	x	0.8384(4)	0.8380(4)	0.8377(4)	0.8379(2)	0.8385(5)
	y	0.0128(3)	0.0123(3)	0.0169(4)	0.0177(2)	0.0157(4)
	z	0.1612(2)	0.1605(2)	0.1610(3)	0.1606(1)	0.1593(3)
	$B/\text{Å}^2$	0.37(1)	0.70(1)	1.00(3)	0.85(1)	0.69(3)
$Y(2)$	SOF Ge	0.973(1)	0.975(1)	0.996(1)	0.995(1)	0.944(3)
	SOF S	0.027(1)	0.025(1)	0.004(1)	0.005(1)	0.056(3)
	x	0.9366(3)	0.9367(3)	0.9316(4)	0.9323(2)	0.9321(4)
	y	0.2116(4)	0.2109(4)	0.2096(5)	0.2094(3)	0.2074(5)
	z	0.5612(2)	0.5614(2)	0.5642(3)	0.5646(1)	0.5640(2)
	$B/\text{Å}^2$	0.37(1)	0.70(1)	1.00(3)	0.85(1)	0.69(3)
$Q(1)$	SOF Ge	0.027(1)	0.025(1)	0.004(1)	0.005(1)	0.056(3)
	SOF S	0.973(1)	0.975(1)	0.996(1)	0.995(1)	0.944(3)
	x	0.9332(9)	0.9340(9)	0.931(1)	0.9285(5)	0.9265(8)
	y	0.212(1)	0.212(1)	0.214(1)	0.2120(7)	0.207(1)
	z	0.0678(5)	0.0675(5)	0.0723(6)	0.0716(3)	0.0703(6)
	$B/\text{Å}^2$	0.37(1)	0.70(1)	1.00(3)	0.85(1)	0.69(3)
$Q(2)$	SOF Ge	0.027(1)	0.025(1)	0.004(1)	0.005(1)	0.056(3)
	SOF S	0.973(1)	0.975(1)	0.996(1)	0.995(1)	0.944(3)
	x	0.8394(9)	0.837(1)	0.834(1)	0.8366(6)	0.837(1)
	y	0.0195(7)	0.0190(8)	0.0237(9)	0.0249(5)	0.0246(9)
	z	0.6657(6)	0.6659(5)	0.6677(8)	0.6664(4)	0.6652(7)
	$B/\text{Å}^2$	0.37(1)	0.70(1)	1.00(3)	0.85(1)	0.69(3)
Weight percentage (%)		1.61(6) GeO$_2$	2.17(4) GeO$_2$	2.86(8) GeO$_2$	2.54(3) GeO$_2$	3.00(8) Ir
		5.0(7) CoS	3.4(3) CoS	2.3(3) RhS$_2$	2.7(1) RhS$_2$	10.8(2) IrGe
R_{wp} 180° bank (%)		7.7	5.4	10.1	5.9	5.5
R_{wp} 90° bank (%)		4.6	3.1	6.3	4.1	4.3
χ^2		4.8	2.6	2.0	1.4	3.2

The weight percentages of other phases included in the Rietveld refinements are shown.

[a] $M(1)$ on 6(c) (0,0,z); the remaining atoms on 18(f) (x,y,z).

can be calculated from the M–X–M angle using the relationship [27]

$$\cos(M-X-M) = 1 - \frac{2x^2}{9}, \quad \text{where } x = 2\cos\phi + 1.$$

Using this expression on the average M–X–M angle found for the $M\text{Ge}_{1.5}\text{S}_{1.5}$ phases, we have estimated tilt angle values of 35.4°, 37.2° and 37.0° for $M = $ Co, Rh and Ir, respectively. These angles are comparable to those found in binary skutterudites, and follow a similar trend: for a given "anion" the tilt angle increases with increasing the size of the cation [4,27]. The empty A-sites retain the icosahedral coordination found in filled skutterudites, but are slightly distorted. The A–X distances for a hypothetical filler atom A would take an approximate value of 3.1 Å, similar to those found in filled phosphides such as LaFe$_4$P$_{12}$ [6]. This suggests that it may be possible to fill

the A-site of the $M\text{Ge}_{1.5}\text{S}_{1.5}$ phases and is supported by recent reports on the synthesis of the closely related filled skutterudites $A_x\text{Co}_4\text{Ge}_6Q_6$ ($A = $ Ce, Yb; $Q = $ Se, Te) [28,29].

Owing to the tilting of the octahedra, the anions form two-crystallographically distinct four-membered rings, with stoichiometry [Ge$_2$S$_2$]$^{4-}$, in which the germanium and sulphur atoms are *trans* to each other. The intraring Ge–S distances (Table 3) are comparable to those found in binary germanium sulphides, such as GeS (2.44 Å) [30] or GeS$_2$ (2.21 Å) [31]. In addition to the intraring contacts, each Ge and S atom on a Ge$_2$S$_2$ ring has two short contacts with an adjacent ring, of ca. 3.1 Å, which are shorter than the sum of the van der Waals' radii [32]. Early work suggested that the structures of skutterudites followed the so-called Oftedal's relation ($y + z = \frac{1}{2}$, where y and z are the atomic coordinates of X in $Im\bar{3}$), which results in
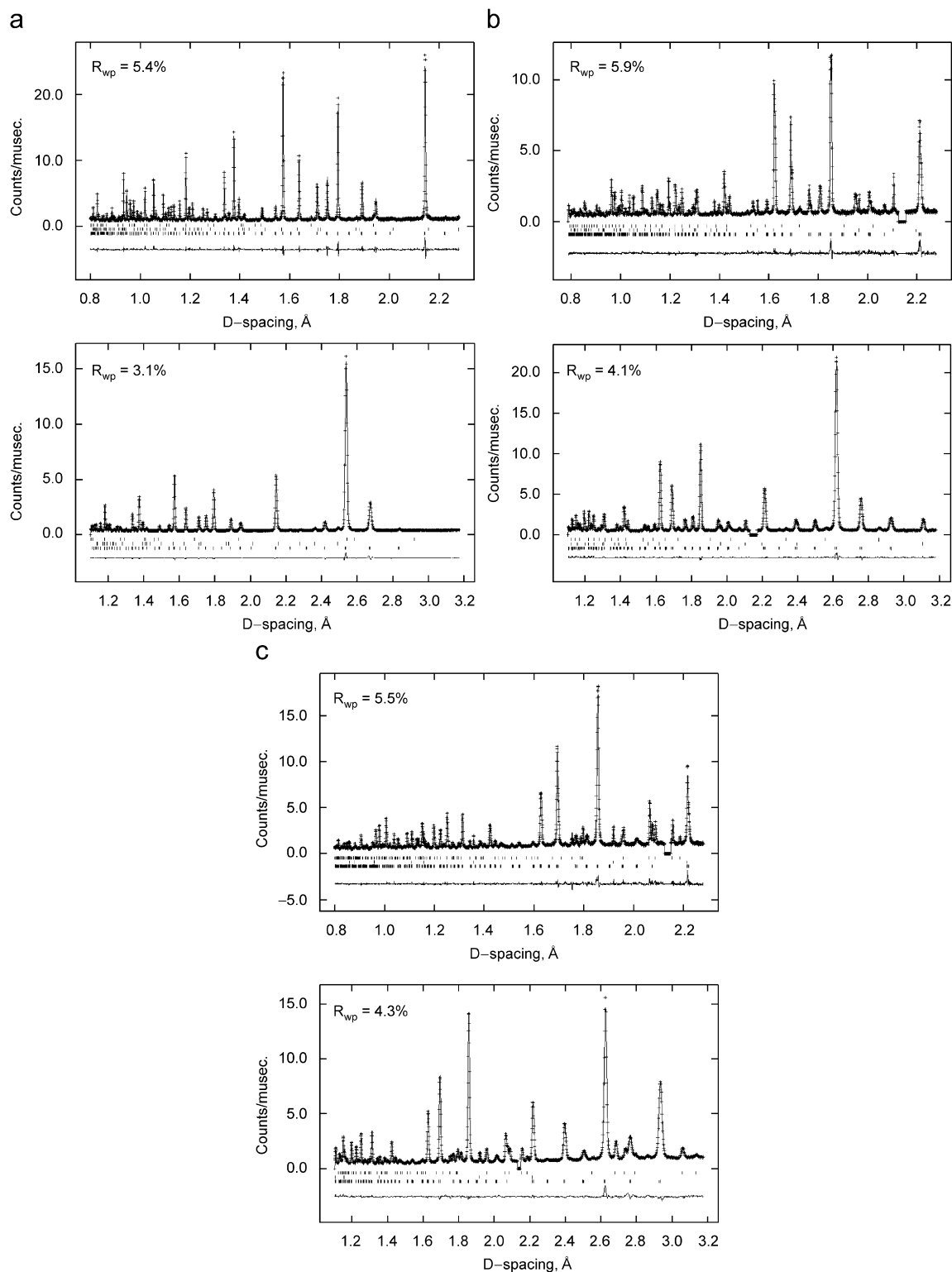
Fig. 2. Observed (crosses), calculated (upper full line) and difference (lower full line) room temperature powder neutron diffraction profiles of (a) $CoGe_{1.5}S_{1.5}$ (lower reflection markers, skutterudite; middle markers, GeO_2; upper markers, CoS); (b) $RhGe_{1.5}S_{1.5}$ (lower markers, skutterudite; middle markers, GeO_2; upper markers, RhS_2); and (c) $IrGe_{1.5}S_{1.5}$ (lower markers, skutterudite; middle markers, Ir; upper markers, IrGe). Data were collected in the backscattering detector banks (upper plot) and in the 90° bank (lower plot). All refinements were carried out in the space group $R\bar{3}$.

squared X_4 rings. However subsequent structural studies revealed that in the vast majority of filled and unfilled skutterudites the X_4 rings are instead rectangular, with short and long X–X distances alternating within the ring. The largest distortions of the X_4 rings are found in unfilled skutterudites, with the rings becoming squarer as the filling

Table 3
Selected bond distances (Å) and angles (deg) for the $MY_{1.5}Q_{1.5}$ phases

|	CoGe$_{1.5}$S$_{1.5}$		RhGe$_{1.5}$S$_{1.5}$		IrGe$_{1.5}$S$_{1.5}$
	4.2 K	293 K	4.2 K	293 K	293 K
$M(1)$–$Y(1)$	2.335(9) × 3	2.341(9) × 3	2.390(7) × 3	2.393(4) × 3	2.407(5) × 3
$M(1)$–$Q(2)$	2.207(12) × 3	2.230(12) × 3	2.386(12) × 3	2.386(6) × 3	2.384(11) × 3
$Y(1)$–$M(1)$–$Y(1)$	89.9(4) × 3	90.0(4) × 3	92.98(30) × 3	93.13(14) × 3	91.63(18) × 3
$Y(1)$–$M(1)$–$Q(2)$	86.46(22) × 3	86.32(22) × 3	85.22(27) × 3	85.83(14) × 3	86.74(26) × 3
	84.10(19) × 3	84.05(19) × 3	83.05(23) × 3	83.45(12) × 3	83.83(21) × 3
$Q(2)$–$M(1)$–$Q(2)$	99.1(4) × 3	99.2(4) × 3	98.6(4) × 3	97.50(20) × 3	97.64(32) × 3
$M(2)$–$Y(1)$	2.360(13)	2.339(13)	2.359(10)	2.379(5)	2.375(6)
$M(2)$–$Y(2)$	2.282(10)	2.300(10)	2.390(9)	2.374(4)	2.389(5)
	2.296(7)	2.311(8)	2.377(7)	2.399(3)	2.381(4)
$M(2)$–$Q(1)$	2.271(10)	2.262(11)	2.410(12)	2.382(6)	2.378(9)
	2.303(13)	2.283(14)	2.394(12)	2.436(7)	2.461(9)
$M(2)$–$Q(2)$	2.241(16)	2.248(16)	2.423(14)	2.421(7)	2.411(11)
$Y(1)$–$M(2)$–$Y(2)$	83.82(28)	84.02(23)	85.37(20)	85.38(11)	86.17(17)
	83.19(30)	83.54(25)	84.42(25)	84.27(12)	84.91(17)
$Y(1)$–$M(2)$–$Q(1)$	94.1(5)	94.3(5)	97.3(4)	97.26(21)	96.34(29)
	90.8(7)	91.6(6)	94.2(6)	93.60(28)	92.3(4)
$Y(2)$–$M(2)$–$Y(2)$	92.1(4)	91.3(4)	93.15(35)	93.13(17)	92.60(22)
$Y(2)$–$M(2)$–$Q(1)$	87.8(4)	87.68(34)	86.3(4)	87.21(20)	88.15(32)
	83.10(28)	83.66(28)	82.11(28)	82.01(15)	83.61(24)
$Y(2)$–$M(2)$–$Q(2)$	97.9(7)	97.2(6)	97.5(5)	97.55(25)	97.08(31)
	95.5(5)	94.9(5)	95.2(4)	94.13(17)	94.57(28)
$Q(1)$–$M(2)$–$Q(1)$	96.7(6)	97.2(6)	98.4(6)	97.66(29)	95.7(4)
$Q(1)$–$M(2)$–$Q(2)$	87.2(4)	87.3(4)	83.2(4)	83.27(22)	84.15(34)
	87.5(5)	87.1(4)	82.9(4)	83.40(22)	84.4(4)
$Y(1)$–$Q(1)$	2.345(11)	2.350(11)	2.368(15)	2.349(7)	2.335(13)
	2.548(10)	2.567(10)	2.518(14)	2.523(7)	2.592(12)
$Q(1)$–$Y(1)$–$Q(1)$	87.13(27)	87.42(27)	86.71(31)	86.72(17)	85.99(28)
$Y(2)$–$Q(2)$	2.378(10)	2.380(10)	2.397(12)	2.374(6)	2.362(11)
	2.547(10)	2.541(9)	2.486(12)	2.486(12)	2.555(11)
$Q(2)$–$Y(2)$–$Q(2)$	87.35(27)	87.17(27)	86.59(29)	86.61(17)	86.60(27)
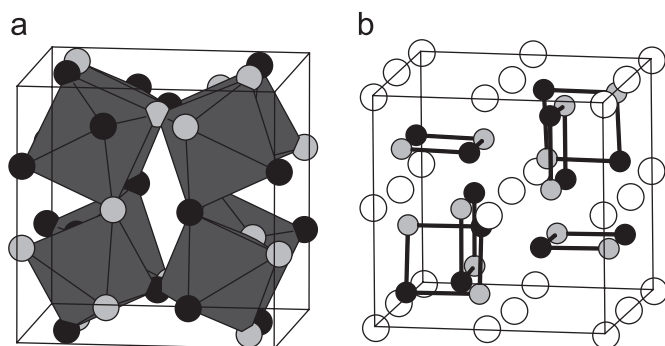
Fig. 3. (a) Polyhedral representation and (b) ball-and-stick representation of the structure of the ordered skutterudite CoGe$_{1.5}$S$_{1.5}$ showing the anion ordering. For comparison purposes with Fig. 1(c), the rhombohedral setting has been used. Key: cobalt, open circles; sulphur, grey circles; germanium, black circles.

fraction increases [8]. While in unfilled binary skutterudites the ratio between the X–X distances takes typically values between 1.03 and 1.05 [2], in the MGe$_{1.5}$S$_{1.5}$ phases, this ratio ranges between 1.06 and 1.11. In addition, the S–Ge–S angles within the rings lie over the range 85.99(28)–87.42(27)$^{\circ}$, while the Ge–S–Ge angles are greater than 90°, indicating that the four-membered rings in the MGe$_{1.5}$S$_{1.5}$ phases are diamond-like instead of rectangular. Molecular-orbital calculations reveal that the substitution of homononuclear X_4 rings by heteronuclear Ge$_2Q_2$ (Q = S, Se) rings in the skutterudite structure, results in changes in the electron distribution within the available π-type orbitals of the rings, owing to the different atomic potentials of Ge and Q [33]. As a consequence, low electron density perpendicular to the ring plane is predicted for the Ge atoms, resulting in stronger covalent bonds between the Ge and the metal atoms than those between the chalcogen and the metal atoms.

3.2. Transport properties

The electrical resistivity of the MGe$_{1.5}$S$_{1.5}$ phases increases with decreasing temperature, indicating that these materials are semiconductors (Fig. 4(a)). The activation energies determined over the high-temperature region of our data using an Arrhenius law (Table 4) are comparable with those previously reported for other ternary phases, such as CoGe$_{1.5}$Se$_{1.5}$ (0.168 eV) [34], IrGe$_{1.5}$S$_{1.5}$ (0.11 eV) [16] or CoGe$_{1.5}$Te$_{1.5}$ (0.16 eV) [20]. For binary skutterudites, which exhibit similar activation energies over this temperature range, it has been suggested that this energy
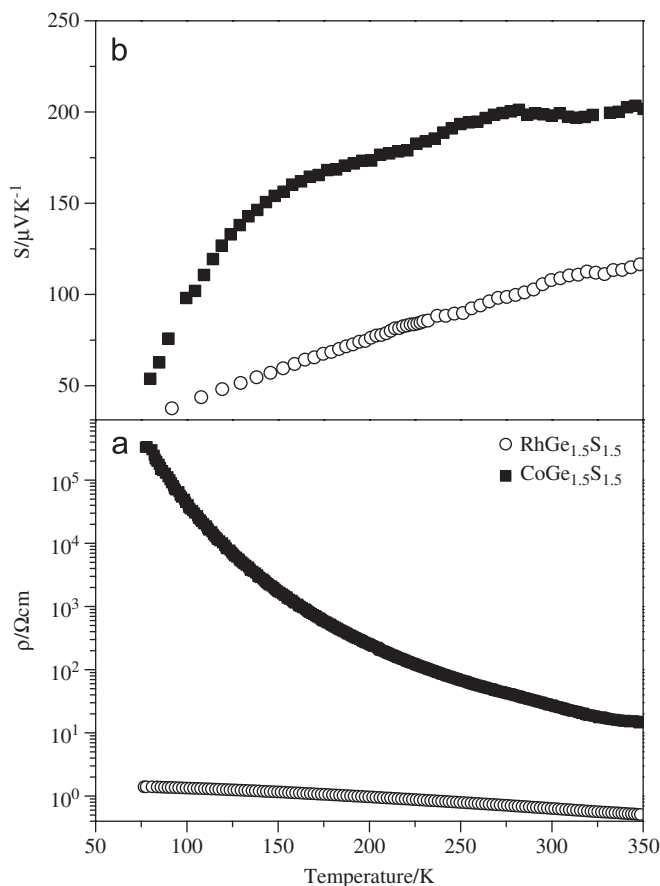
Fig. 4. Temperature dependence of the (a) electrical resistivity and (b) the Seebeck coefficient of $MGe_{1.5}S_{1.5}$ phases.

Table 4
Activation energies derived from the resistivity data using the Arrhenius law

Sample	Temperature range (K)	E_a (eV)	Temperature range (K)	E_a (eV)
$CoGe_{1.5}S_{1.5}$	77–120	0.072(1)	135–350	0.108(1)
$Co_{0.95}Fe_{0.05}Ge_{1.5}S_{1.5}$	77–130	0.030(1)	190–360	0.114(1)
$Co_{0.90}Fe_{0.10}Ge_{1.5}S_{1.5}$	77–120	0.013(1)	190–400	0.059(1)
$RhGe_{1.5}S_{1.5}$	77–125	$2.0(1)\,10^{-3}$	250–350	0.033(1)

represents the activation energy of the extrinsic charge carriers [35]. Therefore measurements at elevated temperatures may be required to determine the intrinsic band gap. The electrical resistivities of these ternary skutterudites are significantly higher than those found for the binary phases [9]. Although higher resistivities can be attributed to lower charge-carrier mobilities, the high resistivity is due primarily to low charge-carrier density which can be increased by doping. As shown in Fig. 5(a), the electrical resistivity of $CoGe_{1.5}S_{1.5}$ can be reduced from $30.6\,\Omega\,cm$ at room temperature to $0.14\,\Omega\,cm$ by doping this material with 10% iron. Doping of the isostructural $CoGe_{1.5}Se_{1.5}$ with nickel also results in a marked decrease of the electrical resistivity [36]. Although on the basis of these
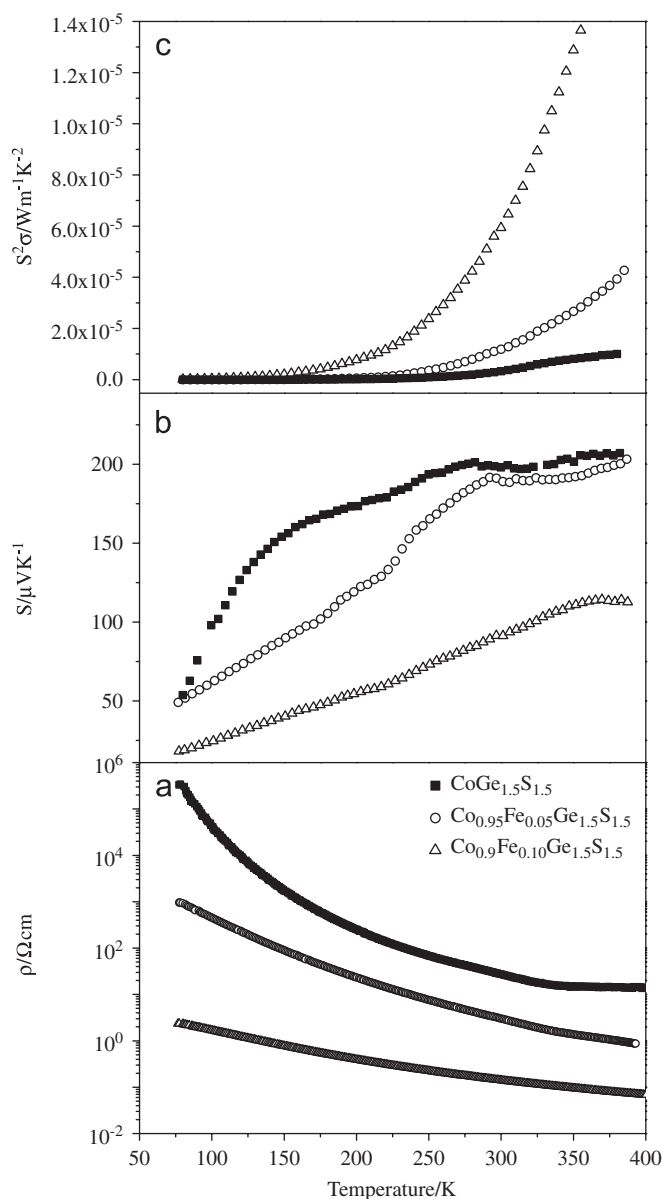

Fig. 5. Temperature dependence of the (a) electrical resistivity, (b) the Seebeck coefficient, and (c) the power factor of $Co_{1-x}Fe_xGe_{1.5}S_{1.5}$ phases.

results optimising the charge-carrier density by doping seems a feasible approach, our doped ternary skutterudites remain quite resistive when compared with their binary counterparts, and further optimisation of the charge-carrier density will be required to improve the thermoelectric properties.

The magnitude of the Seebeck coefficient is also consistent with semiconducting behaviour (Fig. 4(b)), and the positive values found for all samples indicate that the majority of the charge carriers are holes. As previously reported for $CoSb_3$ [9,10], iron acts as a p-type dopant while nickel behaves as an electron donor in the related $CoGe_{1.5}Se_{1.5}$ [36]. Doping with iron in the $Co_{1-x}Fe_x Ge_{1.5}S_{1.5}$ phases (Fig. 5(b)), results in a decrease of the Seebeck coefficient with increasing iron content. For both the undoped and the doped samples, the absolute value of

the Seebeck coefficient increases with temperature in an approximately linear fashion. The binary phase from which these materials can be derived, $CoSb_3$, shows a similar temperature dependence at low temperatures. It has been proposed that the transport properties of $CoSb_3$ below 600 K are characteristic of transport in a band formed by shallow impurity levels, while at elevated temperatures, conduction by intrinsic charge carriers dominates [37]. This is reflected in the temperature dependence of the Seebeck coefficient, which increases with increasing temperature in the extrinsic region, and then starts to decrease in the intrinsic region due to the increasing number of minority carriers [38].

The power factor, $S^2\sigma$, of the $Co_{1-x}Fe_xGe_{1.5}S_{1.5}$ phases (Fig. 5(c)) rises with increasing temperature and with increasing iron content. Whilst the power factor is of the same order of magnitude than those reported for other ternary skutterudites [20,34], it is markedly lower than power factors found in state-of-the-art thermoelectric materials (typically $1 \times 10^{-3}\,Wm^{-1}\,K^{-2}$), owing the higher resistivities that these ternary phases exhibit. However, our initial results indicate that significant improvements of the thermoelectric properties can be achieved by doping these ternary skutterudites, and therefore further studies to optimise the charge-carrier density are of interest.

Extended Hückel tight-binding calculations [39,40] indicate that the presence of X_4 rings in the skutterudite structure is a key feature in determining the nature of the electronic bands and therefore the transport properties of these materials. In particular, it has been reported that the high-energy region of the valence band is mainly formed by bonding and nonbonding π-type X_4 orbitals, while the bottom of the conduction band is mainly formed by antibonding X_4 orbitals. The ordering of anions found in $MGe_{1.5}S_{1.5}$ is therefore likely to have a very significant effect on the band structure of these phases, as suggested by the molecular-orbital calculations on Ge_2Q_2 ($Q = S$, Se) rings of Partik and Lutz [33]. Theoretical studies on the lattice dynamics of $CoSb_3$ also indicate that acoustic and optic phonon modes dominated by substantial Sb motion, and in particular those associated with the Sb_4 ring motion [41], play an important role in the thermal conduction. In $MGe_{1.5}S_{1.5}$, anion-ordering results in a significant increase of the number of lattice vibrations, as evidenced by comparison of the reported infrared spectra of $CoAs_3$ with those of the ternary skutterudites $MGe_{1.5}Q_{1.5}$ ($Q = S$, Se) [17]. This is a consequence of the lower crystal symmetry of the latter ($R\bar{3}$ vs. $Im\bar{3}$), and will have a major effect on the phonon dispersion curves and in the corresponding phonon density of states (DOS), therefore altering the thermal transport behaviour. In addition, the partial disorder of Ge and S atoms between the four available anion sites found in our structural study may result in lower thermal conductivities owing to alloy scattering. Preliminary measurements carried by us on $CoGe_{1.5}S_{1.5}$, using a laser flash method, indicate that this material exhibits a thermal conductivity of $1.9\,Wm^{-1}\,K^{-1}$ at 320 K,

markedly lower than that of $CoSb_3$ ($10.5\,Wm^{-1}\,K^{-1}$) [9], and comparable to reported values for other ternary skutterudites of the type $MY_{1.5}Q_{1.5}$ [19].

4. Conclusions

Our structural study indicates that the $MGe_{1.5}S_{1.5}$ phases adopt an ordered skutterudite structure, in which the anions form diamond-like four-membered Ge_2S_2 rings. According to theoretical calculations [39–41], the anion rings of the skutterudite structure play a key role in both the electrical and thermal transport properties, and therefore substitution of homonuclear X_4 rings with ordered heteronuclear Ge_2S_2 rings is likely to have a major effect on the properties of these materials. Experimental data indicate that, in comparison with binary skutterudites, ternary $MY_{1.5}Q_{1.5}$ phases are quite resistive, but also exhibit significantly lower thermal conductivities.

Reference

[1] J. Ackermann, A. Wold, J. Phys. Chem. Solids 38 (1977) 1013–1016.
[2] A. Kjekshus, T. Rakke, Acta Chem. Scand. A 28 (1974) 99–103.
[3] S. Rundqvist, N.-O. Ersson, Ark. Kemi. 30 (1968) 103–114.
[4] R.H. Mitchell, Perovskites: Modern and Ancient, Almaz Press, Canada, 2002.
[5] B. Bochu, M.N. Deschizeaux, J.C. Joubert, A. Collomb, J. Chevanas, M. Marezio, J. Solid State Chem. 29 (1979) 291–298.
[6] W. Jeitschko, D. Braun, Acta Crys. B 33 (1977) 3401–3406.
[7] F. Grandjean, A. Gérard, D.J. Braun, W. Jeitschko, J. Phys. Chem. Solids 45 (1984) 877–886.
[8] B.C. Chakoumakos, B.C. Sales, J. Alloys Compds. 407 (2006) 87–93.
[9] C. Uher, in: M.G. Kanatzidis, S.D. Mahanti, T.P. Hogan (Eds.), Chemistry, Physics and Materials Science of Thermoelectric Materials: Beyond Bismuth Telluride, Kluwer Academics/Plenum Publishers, New York, 2003, p. 121.
[10] C. Uher, in: D.M. Rowe (Ed.), Thermoelectrics Handbook. Macro to Nano, CRC Press, Boca Raton, 2006 Chapter 34.
[11] B.C. Sales, D. Mandrus, R.K. Williams, Science 272 (1996) 1325–1328.
[12] C. Sekine, T. Uchiumi, I. Shirotani, T. Yagi, Phys. Rev. Lett. 79 (1997) 3218–3221.
[13] I. Shirotani, T. Uchiumi, K. Ohno, C. Sekine, Y. Nakazawa, K. Kanoda, S. Todo, T. Yagi, Phys. Rev. B 56 (1997) 7866–7869.
[14] R. Korenstein, S. Soled, A. Wold, G. Collin, Inorg. Chem. 16 (1977) 2344–2346.
[15] A. Kjekshus, D.G. Nicholson, T. Rakke, Acta Chem. Scand. 27 (1973) 1315–1320.
[16] A. Lyons, R.P. Gruska, C. Case, S.N. Subbarao, A. Wold, Mater. Res. Bull. 13 (1978) 125–128.
[17] H.D. Lutz, G. Kliche, J. Solid State Chem. 40 (1981) 64–68.
[18] T. Caillat, J. Kulleck, A. Borshchevsky, J.-P. Fleurial, J. Appl. Phys. 79 (1996) 8419–8426.

[19] J.-P. Fleurial, T. Caillat, A. Borshchevsky, in: Proceedings of the 16th International Conference on Thermoelectrics, Dresden, Germany, 1997, pp. 1–11.

[20] P. Vaqueiro, G.G. Sobany, A.V. Powell, K.S. Knight, J. Solid State Chem. 179 (2006) 2047–2053.

[21] W.I.F. David, M.W. Johnson, K.J. Knowles, C.M. Moreton-Smith, G.D. Crisbie, E.P. Campbell, S.P. Graham, J.S. Lyall, Rutherford Appleton Laboratory Report, RAL-86-102, 1986.

[22] A.C. Larson, R.B. von Dreele, General Structure Analysis System, Los Alamos Laboratory, [Report LAUR 85-748], 1994.

[23] M. Partik, C. Kringe, H.D. Lutz, Z. Kristallogr. 211 (1996) 304–312.

[24] A.L. Spek, J. Appl. Cryst. 36 (2003) 7–13.

[25] A.L. Spek, J. Appl. Cryst. 21 (1988) 578–579.

[26] R.D. Shannon, Acta Cryst. A 32 (1976) 751–767.

[27] M. O'Keeffe, B.G. Hyde, Acta Cryst. B 33 (1977) 3802–3813.

[28] Q. Lin, A.L.E. Smalley, D.C. Johnson, J. Martin, G.S. Nolas, Chem. Mater. 19 (2007) 6615–6620.

[29] J. Navrátil, T. Plecháček, L. Beneš, M. Vlček, F. Laufek, in: Proceedings of the Fifth European Conference on Thermoelectrics, Odessa, Ukraine, 2007, p. 52.

[30] H. Wiedemeier, H.G. Von Schnering, Z. Kristallogr 148 (1978) 295–303.

[31] G. Dittmar, H. Schaefer, Acta Cryst. B 32 (1976) 1188–1192.

[32] A. Bondi, J. Phys. Chem. 68 (1964) 441–451.

[33] M. Partik, H.D. Lutz, Phys. Chem. Min. 27 (1999) 41–46.

[34] G.S. Nolas, J. Yang, R.W. Ertenberg, Phys. Rev. B 68 (2003) 193206.

[35] E. Arushanov, K. Fess, W. Kaefer, Ch. Kloc, E. Bucher, Phys. Rev. B 56 (1997) 1911–1917.

[36] G.S. Nolas, M. Beekman, R.W. Ertenberg, J. Yang, J. Appl. Phys. 100 (2006) 036101.

[37] J.W. Sharp, E.C. Jones, R.K. Williams, P.M. Martin, B.C. Sales, J. Appl. Phys. 78 (1995) 1013–1018.

[38] T. Caillat, A. Borshchevsky, J.-P. Fleurial, J. Appl. Phys. 80 (1996) 4442–4449.

[39] D. Jung, M.-H. Whangbo, S. Alvarez, Inorg. Chem. 29 (1990) 2252–2255.

[40] M. Llunell, P. Alemany, S. Alvarez, V.P. Zhukov, A. Vernes, Phys. Rev. B 53 (1996) 10605–10609.

[41] J.L. Feldman, D.J. Singh, Phys. Rev. B 53 (1996) 6273–6282.